

Synthesis and Structural Characterization of a Cu(II) Coordination Polymer from N^1, N^2 -Di(pyridin-4-yl)oxalamide

Hai-Wei Kuai, Tao Hu, Ding-Yun Jiang,
Yun-Hua Qian, and Deng-Hao Li

Faculty of Life Science and Chemical Engineering,
Huaiyin Institute of Technology, Huaian 223003, China

Reprint requests to Dr. Hai-Wei Kuai. Fax:
+86-517-83559044. E-mail: hytshy@126.com

Z. Naturforsch. **2014**, *69b*, 1045–1049

DOI: 10.5560/ZNB.2014-4142

Received July 4, 2014

The reaction of $\text{Cu}(\text{NO}_3)_2 \cdot 3\text{H}_2\text{O}$ with N^1, N^2 -di(pyridin-4-yl)oxalamide (L) and KSCN in the presence of DMF by the layering method gives rise to a new complex $[\text{Cu}(\text{L}_2)(\text{SCN})_2(\text{DMF})_2]_n$ (**1**). Complex **1** has been characterized by single-crystal and powder X-ray diffraction, IR spectroscopy, and elemental and thermogravimetric analyses. It crystallizes in the triclinic system with space group $P\bar{1}$ and shows a chain structure. Delicate N–H...O hydrogen bonding exists in individual units, and adjacent chains are linked by intermolecular interactions, resulting in an extended 2D network.

Key words: Cu(II), Coordination Polymer, Structural Characterization

Introduction

The rational design and synthesis of coordination frameworks have recently attracted remarkable attention in view of their diverse structures and topologies as well as potential applications in many fields such as heterogeneous catalysis, ion-recognition, nonlinear optics, and molecular adsorption [1–3]. Up to now, a great number of metal-organic frameworks (MOFs) have been deliberately prepared [4–6]. The assembling strategies of coordination architectures involve the design of organic building blocks and the employment of certain metal centers [7–9]. Hitherto, extensive research has been carried out to manage these factors, including the coordination geometry of the metal center, the intrinsic nature of the organic ligand, and experimental conditions such as acidic or basic media for the re-

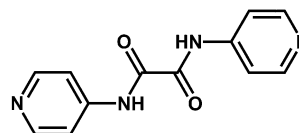


Fig. 1. Schematic drawing of the ligand L.

action system, reaction solvent, and temperature, as well as the metal-to-ligand ratio to achieve structural diversity [10–12]. Among the above mentioned influential factors, the nature of the organic ligand has been documented as crucial in the formation of supramolecular coordination compounds [13, 14]. Among the much employed organic ligands, *N*- and/or *O*-donor multidentate compounds are regarded as excellent building blocks for the construction of selected frameworks [15, 16].

In our previous study, we used a series of semirigid *N*- and *O*-donor ligands, for example 5-(1*H*-benzotriazol-1-ylmethyl)isophthalic acid, 5-(benzimidazol-1-ylmethyl)isophthalic acid, and 3,5-bis(2-pyridylmethyl)aminobenzoic acid to construct supramolecular coordination compounds [17–19]. Based on these studies, we have recently been focusing our attention on the utilization of the rigid ligand N^1, N^2 -di(pyridin-4-yl)oxalamide (L) as an organic block to react with various metal salts under appropriate synthetic conditions. L is a neutral bidentate ligand (Fig. 1). We aim at employing this ligand to assemble complexes with porous frameworks in the presence of other anions such as SCN^- and N_3^- , which always help to avoid blocking the porous frameworks. The amide moieties $-\text{NH}-\text{CO}-$ in the ligand L are expected to show special affinity to CO_2 gas [20, 21]. Therefore, it can be used in the exploration of gas storage materials. We report herein the synthesis and structural characterization of $[\text{Cu}(\text{L}_2)(\text{SCN})_2(\text{DMF})_2]_n$ (**1**).

Results and Discussion

Preparation

The reaction of $\text{Cu}(\text{NO}_3)_2 \cdot 3\text{H}_2\text{O}$ with N^1, N^2 -di(pyridin-4-yl)oxalamide (L) and KSCN in the presence of DMF *via* the layering method affords the complex $[\text{Cu}(\text{L}_2)(\text{SCN})_2(\text{DMF})_2]_n$ (**1**) which is stable in air.

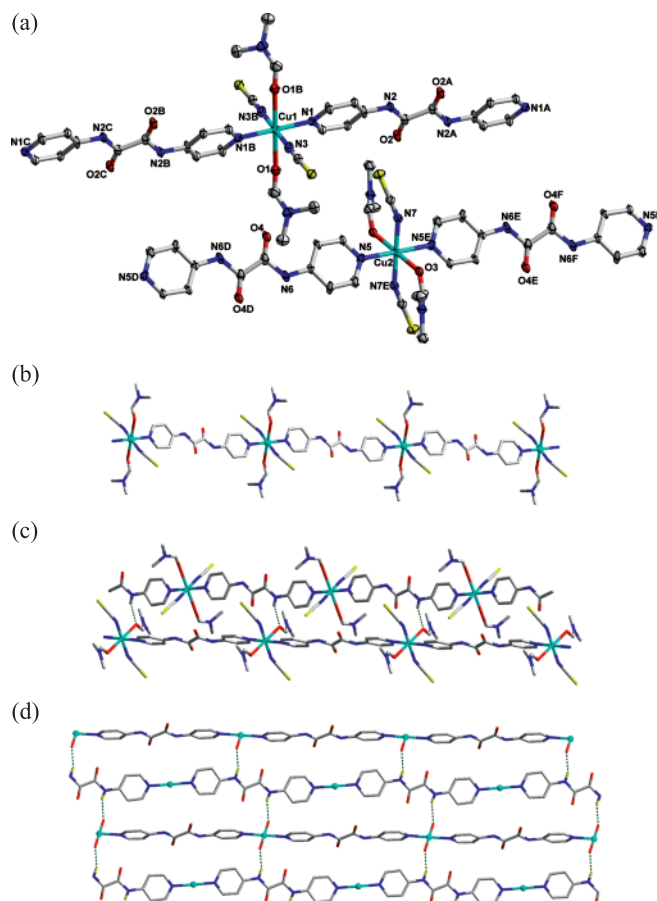


Fig. 2 (color online). (a) The coordination environment of the Cu(II) ions in **1** with displacement ellipsoids drawn at the 30% probability level. The hydrogen atoms are omitted for clarity; (b) the 1D structure of **1**; (c) view of the double-chain structure in **1**; (d) view of the 2D network of **1** extended by hydrogen bonding interactions.

Structural description of $[Cu(L)_2(SCN)_2(DMF)_2]_n$ (**1**)

Determination of the structure of complex **1** by X-ray crystallography has shown that it crystallizes in the triclinic crystal system with space group $P\bar{1}$ and $Z = 2$ (Table 1).

As shown in Fig. 2a, in the asymmetrical unit of complex **1** there are two different Cu atoms (Cu1 and Cu2), two halves of L, two SCN^- , and two DMF molecules. Each Cu(II) cation resides on an inversion center and is six-coordinated by two nitrogen atoms from two different L ligands, two oxygen atoms from two different DMF molecules, and two nitrogen atoms from two coordinated SCN^- anions to furnish an elongated octahedral coordination geometry $[CuN_4O_2]$.

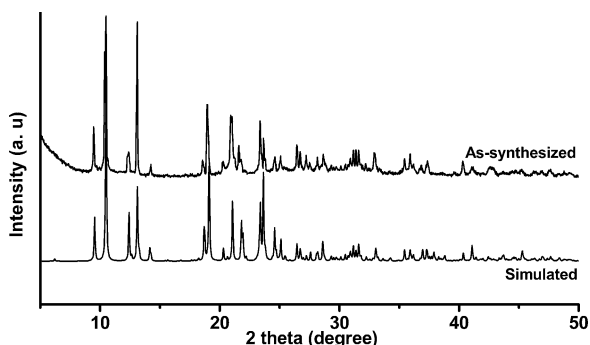
Due to the inversion symmetry, the six coordinating atoms around each Cu(II) cation can be grouped into equivalent sets $[Cu(1)-O(1) = 2.518(3) \text{ \AA}, Cu(1)-N(1) = 2.029(3) \text{ \AA}, Cu(1)-N(3) = 1.941(4) \text{ \AA}]$ and $[Cu(2)-O(3) = 2.486(3) \text{ \AA}, Cu(2)-N(5) = 2.040(3) \text{ \AA}, Cu(2)-N(7) = 1.950(4) \text{ \AA}]$ (Table 2). The Cu–O bonds around each Cu(II) are conspicuous for their distances. These elongated axial lengths may originate from the Jahn-Teller effect based on the consideration of the electronic degenerate ground state of Cu(II) ion with $d^9[(t_{2g})^6(e_g)^3]$ electron configuration [22–26].

The ligand L acts as a linear bidentate bridging ligand. The SCN^- counterions adopt a monodentate coordination mode: N atoms are coordinated, and S atoms are free of coordination. Cu(II) ions and L

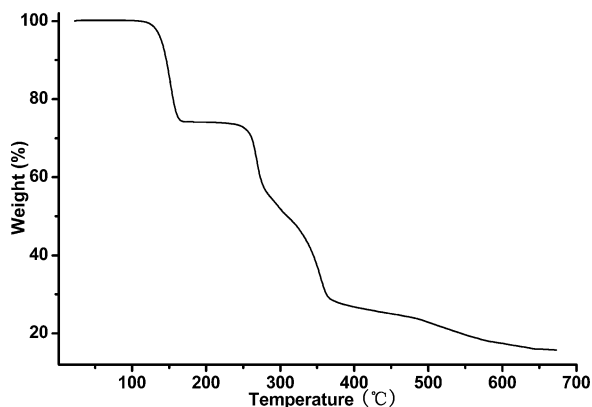
Table 1. Crystal structure data for complex **1**.

Empirical formula	C ₂₀ H ₂₄ N ₈ O ₄ S ₂ Cu
<i>M_r</i>	568.13
Crystal size, mm ³	0.20 × 0.20 × 0.20
Crystal system	triclinic
Space group	<i>P</i> $\bar{1}$
<i>a</i> , Å	9.1258(8)
<i>b</i> , Å	10.0512(9)
<i>c</i> , Å	15.5257(14)
α , deg	108.8310(10)
β , deg	100.334(2)
γ , deg	98.9100(10)
<i>V</i> , Å ³	1290.9(2)
<i>Z</i>	2
<i>D</i> _{calcd.} , g cm ⁻³	1.46
μ (Mo <i>K</i> α), cm ⁻¹	1.1
<i>F</i> (000), e	586
<i>hkl</i> range	-11 → +6, \pm 12, -19 → +18
θ _{max} , deg	2.15–25.80
Refl. measured/unique/ <i>R</i> _{int}	6983/4860/0.0035
Param. refined	323
<i>R</i> 1 (<i>F</i>) ^a / <i>wR</i> 2 (<i>F</i> ²) ^b (all refls.)	0.0648/0.1441
GoF (<i>F</i> ²) ^c	1.025
$\Delta\rho$ _{fin} (max/min), e Å ⁻³	0.49/–0.40

^a $R1 = \sum ||F_o| - |F_c|| / \sum |F_o|$; ^b $wR2 = [\sum w(F_o^2 - F_c^2)^2 / \sum w(F_o^2)^2]^{1/2}$, $w = [\sigma^2(F_o^2) + (AP)^2 + BP]^{-1}$, where $P = (\text{Max}(F_o^2, 0) + 2F_c^2)/3$; ^c $\text{GoF} = [\sum w(F_o^2 - F_c^2)^2 / (n_{\text{obs}} - n_{\text{param}})]^{1/2}$.

Fig. 3. Calculated and observed PXRD patterns of complex **1**.

ligands are interconnected to yield a 1D structure (Fig. 2b). Among adjacent chains, the Cu...Cu separation amounts to 8.269 Å. Apart from coordinative bonding, hydrogen bonds are available in the complex (Table 3). In the crystal, there exist two different chains (one contains Cu1 and the other one Cu2), which are extended into double-chains through N(2)–H(2N)...O(3) interaction (Fig. 2c). An extended 2D network is formed by further interlinkage of the double-chains (Fig. 2d).

Fig. 4. TGA curves of complex **1**.Table 2. Selected bond lengths (Å) and angles (deg) for complex **1**^a.

Cu(1)–O(1)	2.518(3)	Cu(2)–O(3)	2.486(3)
Cu(1)–N(3)	1.940(4)	Cu(1)–N(1)	2.029(3)
Cu(2)–N(5)	2.039(3)	Cu(2)–N(7)	1.950(4)
O(1)–Cu(1)–N(1)	90.41(13)	O(3)–Cu(2)–N(5)	90.83(11)
O(1)–Cu(1)–N(3)	92.12(14)	N(5)–Cu(2)–N(7)	90.30(14)
O(1)–Cu(1)–N(3)#1	87.88(14)	O(3)–Cu(2)–N(7)	89.73(13)
N(1)–Cu(1)–N(3)#1	89.79(14)	O(1)–Cu(1)–N(1)#1	89.59(13)
O(3)–Cu(2)–N(5)#2	89.17(11)	O(3)–Cu(2)–N(7)#2	90.27(13)
N(5)–Cu(2)–N(7)#2	89.71(14)		

^a Symmetry transformations used to generate equivalent atoms: #1 $-x, 1-y, 1-z$; #2 $1-x, 1-y, -z$.

Table 3. Hydrogen bonding data for complex **1**^a.

D–H...A	<i>d</i> (D...A) (Å)	\angle D–H...A (deg)
[Cu(L ₂)(SCN) ₂ (DMF) ₂] _{<i>n</i>} (1)		
N(2)–H(2N)...O(2)#1	2.689(4)	107
N(2)–H(2N)...O(3)#2	3.005(5)	157
N(6)–H(6N)...S(1)#3	3.624(4)	154
N(6)–H(6N)...O(4)#4	2.687(4)	108

^a Symmetry transformations used to generate equivalent atoms: #1 $-1-x, -y, -z$; #2 $-x, 1-y, -z$; #3 $1+x, y, z$; #4 $2-x, 2-y, 1-z$.

PXRD and thermal stability of complex **1**

The phase purity of **1** could be proven by powder X-ray diffraction (PXRD). As shown in Fig. 3, the PXRD pattern of the as-synthesized sample is consistent with the simulated one.

Thermogravimetric analysis (TGA) was carried out for complex **1**, and the result is shown in Fig. 4. There is a steep weight loss of 25.5% from 116 to 166 °C corresponding to the release of coordinated DMF molecules (calcd. 25.7%). The decomposition of

the framework of **1** can be observed at 245 °C. The continuous decomposition terminates at 650 °C with a total weight loss of 85.8%, which is in agreement with the total weight loss calculated for the decomposition leading to the formation of CuO (86.0%) as final residual.

Experimental Section

All commercially available chemicals were of reagent grade and used as received without further purification. The ligand L was synthesized *via* the experimental procedure reported in the literature [27]. Its crystal structure has been reported previously [28]. Elemental analyses of C, H, and N were taken on a Perkin-Elmer 240C elemental analyzer. Infrared spectra (IR) were recorded on a Bruker Vector22 FT-IR spectrophotometer using KBr pellets. Thermogravimetric analysis (TGA) was performed on a simultaneous SDT 2960 thermal analyzer under nitrogen atmosphere with a heating rate of 10 °C min⁻¹. Powder X-ray diffraction (PXRD) patterns were measured on a Shimadzu XRD-6000 X-ray diffractometer with CuK α ($\lambda = 1.5418 \text{ \AA}$) radiation at room temperature.

Preparation of [Cu(L₂)(SCN)₂(DMF)₂]_n (**1**)

The title complex was prepared by the layering method. A buffer layer of a CH₃OH/DMF (1 : 1) solution (8 mL) was carefully layered over a solution of L (24.1 mg, 0.1 mmol) and KSCN (9.7 mg, 0.1 mmol) in DMF (5 mL). Then a solution of Cu(NO₃)₂·3H₂O (12.5 mg, 0.05 mmol) in CH₃OH (3 mL) was layered over the buffer layer. Green block-shaped crystals were obtained after 2 weeks in 60% yield based on L. – C₂₀H₂₄N₈O₄S₂Cu (568.13): calcd. C 42.28, H 4.26, N

19.72; found C 42.16, H 4.45, N 19.90%. – IR (KBr pellet, cm⁻¹): $\nu = 3336$ (m), 2098 (s), 1709 (s), 1658 (m), 1613(s), 1580 (s), 1512 (s), 1484 (s), 1421 (s), 1393 (w), 1333 (s), 1284 (m), 1211 (s), 1146 (m), 1105 (w), 1064 (w), 1022 (m), 881 (m), 827 (m), 799 (w), 658 (m), 552 (m), 493 (m).

X-Ray structure determination

The crystallographic data collection for complex **1** was carried out on a Bruker Smart ApexII CCD area detector diffractometer using graphite-monochromatized MoK α radiation ($\lambda = 0.71073 \text{ \AA}$) at 293(2) K. The diffraction data were integrated using the program SAINT [29], which was also used for the intensity corrections for Lorentz and polarization effects. Semi-empirical absorption corrections were applied using the program SADABS [30]. The structure of **1** was solved by Direct Methods, and all non-hydrogen atoms were refined anisotropically on F^2 by the full-matrix least-squares techniques using the program SHELXL-97 [31–33]. In **1**, all hydrogen atoms at C atoms were generated geometrically. The hydrogen atoms at N atoms could be found at a reasonable position in the difference Fourier maps. The details of crystal parameters, data collection, and refinements are summarized in Table 1, selected bond lengths and angles are listed in Table 2.

CCDC 1011518 contains the supplementary crystallographic data for this paper. These data can be obtained free of charge from The Cambridge Crystallographic Data Centre via www.ccdc.cam.ac.uk/data_request/cif.

Acknowledgement

The authors gratefully acknowledge Huaian Administration of Science & Technology of Jiangsu Province of China (HAG2013019) for financial support of this work.

-
- [1] T. R. Cook, Y. R. Zheng, P. J. Stang, *Chem. Rev.* **2013**, *113*, 734–777.
- [2] T. Uemura, Y. Ono, Y. Hijikata, S. Kitagawa, *J. Am. Chem. Soc.* **2010**, *132*, 4917–4924.
- [3] J. M. Jia, S. J. Liu, Y. Cui, S. D. Han, T. L. Hu, X. H. Bu, *Cryst. Growth Des.* **2013**, *13*, 4631–4634.
- [4] M. L. Wei, X. X. Wang, J. J. Sun, X. Y. Duan, *J. Solid State Chem.* **2013**, *202*, 200–206.
- [5] D. J. Tranchemontagne, J. L. Mendoza-Cortés, M. O’Keeffe, O. M. Yaghi, *Chem. Soc. Rev.* **2009**, *38*, 1257–1283.
- [6] B. L. Chen, S. C. Xiang, G. D. Qian, *Acc. Chem. Res.* **2010**, *43*, 1115–1124.
- [7] L. Luo, G. C. Lv, P. Wang, Q. Liu, K. Chen, W. Y. Sun, *CrystEngComm* **2013**, *15*, 9537–9543.
- [8] L. Luo, K. Chen, Q. Liu, Y. Lu, T. A. Okamura, G. C. Lv, Y. Zhao, W. Y. Sun, *Cryst. Growth Des.* **2013**, *13*, 2312–2321.
- [9] X. C. Cheng, X. H. Zhu, H. W. Kuai, *Z. Naturforsch.* **2012**, *67b*, 1248–1254.
- [10] H. W. Kuai, X. C. Cheng, X. H. Zhu, *Polyhedron* **2013**, *50*, 390–397.
- [11] H. W. Kuai, X. C. Cheng, X. H. Zhu, *Z. Naturforsch.* **2013**, *68b*, 147–154.
- [12] H. W. Kuai, X. C. Cheng, L. D. Feng, X. H. Zhu, *Z. Anorg. Allg. Chem.* **2011**, *637*, 1560–1565.
- [13] P. Wang, L. Luo, J. Fan, G. C. Lv, Y. Song, W. Y. Sun, *Micropor. Mesopor. Mater.* **2013**, *175*, 116–124.

- [14] S. Hazra, S. Bhattacharya, M. K. Singh, L. Carrella, E. Rentschler, T. Weyhermueller, G. Rajaraman, S. Mohanta, *Inorg. Chem.* **2013**, *52*, 12881–12892.
- [15] Z. H. Chen, Y. Zhao, S. S. Chen, P. Wang, W. Y. Sun, *J. Solid State Chem.* **2013**, *202*, 215–226.
- [16] H. W. Kuai, J. Fan, Q. Liu, W. Y. Sun, *CrystEngComm* **2012**, *14*, 3708–3716.
- [17] H. W. Kuai, X. C. Cheng, X. H. Zhu, *Polyhedron* **2013**, *53*, 113–121.
- [18] H. W. Kuai, X. C. Cheng, X. H. Zhu, *J. Coord. Chem.* **2013**, *66*, 28–41.
- [19] H. W. Kuai, X. C. Cheng, X. H. Zhu, *J. Coord. Chem.* **2011**, *64*, 1636–1644.
- [20] M. S. Chen, M. Chen, T. A. Okamura, W. Y. Sun, N. Ueyama, *Micropor. Mesopor. Mater.* **2011**, *139*, 25–30.
- [21] M. S. Chen, Z. S. Bai, T. A. Okamura, Z. Su, S. S. Chen, W. Y. Sun, N. Ueyama, *CrystEngComm* **2010**, *12*, 1935–1944.
- [22] H. Aghabozorg, G. J. Palenik, R. C. Stoufer, J. Summers, *Inorg. Chem.* **1982**, *21*, 3903–3907.
- [23] C. J. Simmons, A. Clearfield, W. Fitzgerald, S. Tyagi, B. J. Hathaway, *Inorg. Chem.* **1983**, *22*, 2463–2466.
- [24] A. Avdeef, J. A. Costamagna, J. P. Fackler, Jr., *Inorg. Chem.* **1974**, *8*, 1854–1863.
- [25] J. P. Fackler, Jr., A. Avdeef, *Inorg. Chem.* **1974**, *8*, 1864–1875.
- [26] R. S. Gall, N. G. Connelly, L. F. Dahl, *J. Am. Chem. Soc.* **1974**, *12*, 4017–4019.
- [27] M. S. Chen, Z. S. Bai, Z. Su, S. S. Chen, W. Y. Sun, *Inorg. Chem. Commun.* **2009**, *12*, 530–533.
- [28] B. C. Tzeng, Y. F. Chen, C. C. Wu, C. C. Hu, Y. T. Chang, C. K. Chen, *New J. Chem.* **2007**, *31*, 202–209.
- [29] SAINT, Program for Data Extraction and Reduction, Bruker Analytical X-ray Instruments Inc., Madison, Wisconsin (USA) **2001**.
- [30] G. M. Sheldrick, SADABS, Program for Empirical Absorption Correction of Area Detector Data, University of Göttingen, Göttingen (Germany) **1997**.
- [31] G. M. Sheldrick, SHELXS/L-97, Programs for Crystal Structure Determination, University of Göttingen, Göttingen (Germany) **1997**.
- [32] G. M. Sheldrick, *Acta Crystallogr.* **1990**, *A46*, 467–473.
- [33] G. M. Sheldrick, *Acta Crystallogr.* **2008**, *A64*, 112–122.